1-1-2009

Stretching induced Hall current and conductance anisotropy in graphene

A R Wright
University of Wollongong

Chao Zhang
University of Wollongong, czhang@uow.edu.au

Stretching induced Hall current and conductance anisotropy in graphene

A. R. Wright and C. Zhang[a)]
School of Engineering Physics, University of Wollongong, New South Wales 2552, Australia

(Received 1 September 2009; accepted 29 September 2009; published online 20 October 2009)

We evaluate the effect of stretching on the optical conductance of graphene. It is found that the low energy (Dirac regime) isotropy that leads to the "universal conductance" is lost. More significantly, due to the loss of C_3 symmetry, a nonzero Hall conductance emerges for stretching along chiral directions, reaching a maximum at a stretching angle of 45°, and being as high as $\sigma_0=e^2/4\hbar$ at van Hove singular point for bond angle changes of about 2°. Our results indicate that the optical properties of graphene can be tuned by a weak mechanical deformation. © *2009 American Institute of Physics*. [doi:10.1063/1.3251074]

Since the initial discovery of graphene flakes in the laboratory in 2003,[1] an impressive body of literature on single layer graphene (SLG) and graphene nanoribbons has appeared.[2,3] Interesting results include the prediction and observation of electron-hole symmetry and half-integer quantum Hall effect,[4–6] finite conductance at zero charge-carrier concentration,[4] the strong suppression of weak localization,[7–9] and, most importantly in the context of this letter, ac and dc universal conductance.[10–12]

The optical conductance of graphene-based systems within the Dirac regime has been a topic of some interest. This is largely due to two factors. First, the Dirac bandstructure is linear. This leads to a constant density of states and constant transition matrix elements, which in turn leads to a constant, or universal, value of the optical conductance ($\sigma_0=e^2/4\hbar$), for as long as the Dirac approximation is valid. The range of energies over which this universal value applies is approximately $0<\epsilon<1$ eV, to within ≈10% of σ_0.[13] This universal conductance is very interesting. For example, it leads to a transmittance which is directly proportional to the fine structure constant. However, the range of energies over which the universal conductance is applicable has also added to the ongoing interest. In particular, the inclusion of the terahertz to far infrared (THz-FIR) spectrum within the universal conductance makes graphene a viable candidate for applications in these important energy ranges.

Several efforts have been made to investigate the optical response of graphene within these energy ranges. The infrared conductance has been theorized and measured extensively.[14,15] The optical conductance of bilayer graphene has been investigated to seek an improved optical response, and several interesting effects in the THz-FIR range have been observed and predicted,[14,16,17] including a low energy anisotropic peak in the longitudinal optical conductance.[18] The optical properties of graphene nanoribbons have also been investigated, and a strong THz-FIR response has been predicted in bilayer ribbons,[19] as well as single layer ribbons within a magnetic field.[20]

For SLG, a potentially very useful property is the universal optical response over notoriously difficult regions of the spectrum to produce and detect. The response is not just universal across a broad range of energies, but also over all chiral directions. The conical Dirac Hamiltonian assures this property. However, in situations where some amount of chiral anisotropy is desired, or a Hall (transverse) response is needed, SLG is, until now, not ideal.

In this letter we investigate both the longitudinal and Hall optical conductance of graphene, which has been stretched along some direction. We find that due to the loss of x-y symmetry under stretching, the conical Dirac bandstructure at the K points has an elliptical rather than a circular cross-section. This leads to a discrepancy between the Fermi velocities along the armchair and zigzag directions, which in turn alters the relative universal conductivities along each direction.

To model stretched graphene, we assume that the bonds will rotate relative to each other, but that the bond length remains constant. This approximation is equivalent to the nearest neighbor approximation where next nearest neighbors are neglected. The nearest neighbors are kept in their energetically minimum configuration but next nearest neighbors are not. For large stretching magnitudes, the next nearest neighbor distance will approach the first, and this approximation will break down. However, graphene is a very stiff material, and breaks long before this condition is met. Therefore we restrict our attention to very small bond bending angles, with no bond rotation exceeding a couple of degrees. So, to model our system, we assume the center point of the three lattice vectors is fixed. If we introduce a pseudoforce F in some direction ϕ such that $0<\phi<\pi/2$, then the three bonds will rotate about the fixed point accordingly. We define the three unit vectors as

$$\delta_1=(\sin\theta_1,-\cos\theta_1)$$

$$\delta_2=[-\cos(\pi/6-\theta_2),\sin(\pi/6-\theta_2)]$$

$$\delta_3=[\cos(\pi/6+\theta_3),\sin(\pi/6+\theta_3)]. \quad (1)$$

These vectors are depicted in Fig. 1. The three rotation angles θ_i are related by the magnitude of the pseudoforce F and its direction ϕ. Since the center point is fixed, the pseudoforce will apply a torque to the bonds such that $\tau_i=\delta_i\times F$. On the other hand because we are stretching the material, the force is applied in both directions, and so the torque will only be applied to the projection of the unit vector onto the force vector $\hat{n}_i=F/|F|\cdot\delta_i$. The latter provides the fraction of the torque that is applicable. The final result will give the angles θ_i in parametric form with ϕ and F being the

a)Electronic mail: czhang@uow.edu.au.

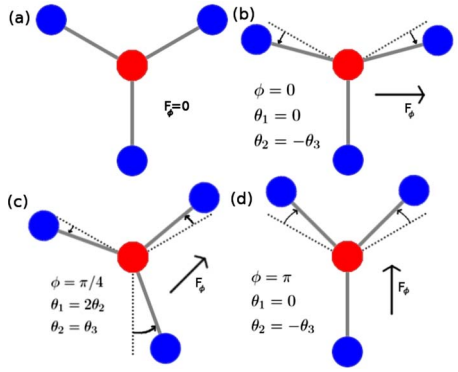

FIG. 1. (Color online) The effect of stretching on the three nearest neighbor bond directions when F is applied along various high symmetry directions. The dotted lines in (b)–(d) are the regular unstretched orientations. The magnitude of F has been chosen to be very large ($F \approx 15$) to emphasize the effect of stretching; however, our numerical results will only go as high as $F=2.5$.

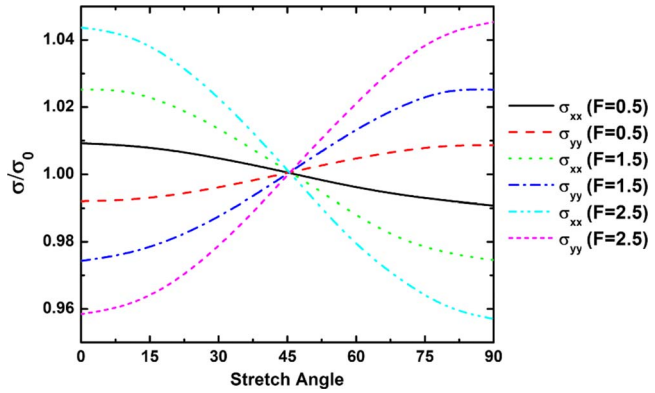

FIG. 2. (Color online) The stretching induced anisotropy in the longitudinal conductance for three small pseudoforce values at $\hbar\omega=0.05t$. These correspond to bond stretching angles of $\approx 0.4°$, 1.2°, and 2° for $F=0.5, 1.5, 2.5$, respectively. Despite the relatively small stretching angle, the induced anisotropy is as much as 10%. The angular dependence of this quantity is quite well behaved. When stretching along the zigzag direction, the zigzag longitudinal conductance is increased, and similarly for stretching along the armchair direction. For stretching of $\pi/4$, the system remains isotropic.

variables $\theta_1 = F \sin 2\phi$, $\theta_2 = F/2(\sin 2\phi + \sqrt{3}\cos 2\phi)$, $\theta_3 = F/2(\sin 2\phi - \sqrt{3}\cos 2\phi)$. The force then, is given by $F = F(\cos\phi, \sin\phi)$.

In Fig. 1, we show the relative rotations of the three bonds at the three most significant (and most symmetric) directions: the zigzag direction ($\phi=0$), the armchair direction ($\phi=\pi/2$), and halfway between the two ($\phi=\pi/4$). As an indication of the magnitude of the effect of F, when stretching along either the zigzag (armchair) direction, $F=1$ corresponds to a rotation of $\pm\sqrt{3}/2°$ of θ_2, where $\theta_3=-\theta_2$.

The tight binding Hamiltonian matrix is

$$H = \begin{pmatrix} 0 & h_{AB} \\ h_{AB}^* & 0 \end{pmatrix}, \tag{2}$$

where $h_{AB}=-t\Sigma_i e^{ik\cdot\hat{\delta}_i}$. Now F is necessarily small as discussed, so we can expand with respect to these terms to obtain

$$\begin{aligned} h_{AB} = &- t\{e^{-ik_y}(1 + iFk_x \sin 2\phi) + 2e^{ik_y/2}[\cos(\sqrt{3}k_x/2) \\ &- iF/4 \cos(\sqrt{3}k_x/2)(k_x \sin 2\phi + 3k_y \cos 2\phi) \\ &- F/4 \sin(\sqrt{3}k_x/2)(\sqrt{3}k_y \sin 2\phi + k_x \cos 2\phi)]\}. \end{aligned} \tag{3}$$

This leads to an energy dispersion of

$$\begin{aligned} \epsilon_s(k) = st[1 &+ 4[\cos^2(\sqrt{3}k_x/2) + \cos 3k_y/2 \cos\sqrt{3}k_x/2] \\ &+ F\{\sin\sqrt{3}k_x(2\cos\sqrt{3}k_x/2 - \cos 3k_y/2) \\ &\times(\sqrt{3}k_y \sin 2\phi + k_x \cos 2\phi) \\ &+ \cos\sqrt{3}k_x/2[(k_x \sin 2\phi + 3k_y \cos 2\phi) \\ &- 4k_x \sin 3k_y/2 \sin 2\phi]\}]^{1/2}. \end{aligned} \tag{4}$$

The eigenvectors can be written in terms of field operators $\Psi_s(r)=(1/4\pi^2)\Sigma_k a_k \phi_s(k) e^{ik\cdot r}$, where $\phi(k)$ is the eigenvalue solution of the Hamiltonian matrix, which is given by $\phi_s(k)^T=(1/\sqrt{2})[sh_{AB}/\epsilon_s(k), 1]$. The current operators are obtained from $J_\nu=\langle\Psi|v_\nu|\Psi\rangle$, where $\nu=x,y$, where $\hat{v}_\nu=\partial H/\partial k_\nu$. The optical conductance is given by Kubo's formula,[21]

$$\sigma_{\mu,\nu}(\omega) = \frac{1}{\omega}\int_0^\infty dt e^{i\omega t}\langle[J_\mu(t), J_\nu(0)]\rangle. \tag{5}$$

The components of the current operator can be calculated from $J_{\nu,\mu}(t)=e^{iHt}J_{\nu,\mu}(0)e^{-iHt}$, where $J_{\nu,\mu}(0)=\Psi^\dagger(r)\hat{v}_{\nu,\mu}\Psi(r')$, in which $\nu,\mu=x,y$. The longitudinal ($\sigma_{\nu\nu}, \nu=x,y$) and Hall (σ_{xy}) optical conductivities are calculated numerically. For our results, we will introduce the dimensionless frequency $\Omega=\hbar\omega/t$, where t is the nearest neighbor hopping integral, and the optical conductivities will be normalized by the "universal" conductance σ_0.

In Fig. 2 we show the longitudinal conductance along the x (zigzag) and y (armchair) directions for various pseudoforce values at $\hbar\omega=0.05t$. While the stretching removes the isotropy of $\sigma_{xx}=\sigma_{yy}$, each component remains approximately universal (frequency independent) for energy up to $\hbar\omega=t$. Beyond this regime the effect of stretching is negligible, and the optical conductance agrees with other calculations for intrinsic graphene.[13] Within the Dirac regime however, we can see that a significant anisotropy develops, which is greatest when the sample is stretched along either the armchair or zigzag directions. When stretched along the zigzag direction ($\phi=0$), the optical conductance along the zigzag direction becomes higher and the conductance along the armchair direction becomes smaller. This discrepancy is as much as $\approx 10\%$ for $F=2.5$, which corresponds to bond bending angles of $\theta_2=-\theta_1\approx 2.16°$. This is a large degree of anisotropy for such a small angle. As the stretching angle changes, we see that at 45° of rotation, the regular isotropic universal conductance is regained. This is not wholly unexpected, but is interesting considering the distortions that graphene obtains on this angle of stretching [see Fig. 1(c)]. As we continue to rotate the angle of stretching, we see that at $\phi=90°$, the reverse situation is obtained as that seen for $\phi=0$.

The Hall conductance for SLG is zero due to the C_3 symmetry of the system. In Fig. 3 we report the variation in the Hall conductance within the Dirac regime as a function of ϕ. We can see that for chiral angles, the Hall conductance is nonzero, reaching a maximum of $\approx\sigma_0/20$ at $\phi=45°$ and $F=2.5$. Despite the broken C_3 symmetry, when stretching along the zigzag or armchair directions, the Hall conductance

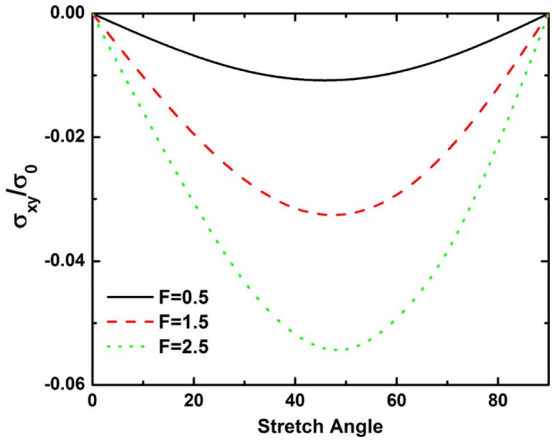

FIG. 3. (Color online) The transverse optical conductance as a function of stretching angle, with $\hbar\omega=0.05t$. Interestingly, even thought the C_3 symmetry is broken for stretching along the high symmetry directions, the transverse conductance remains zero. For chiral stretching this is not the case. Maximum stretching is reached for the longitudinally isotropic value of $\phi=\pi/4$.

still gives zero. The magnitude of the Hall conductance increases linearly with F for small magnitudes of F.

Finally, in Fig. 4 we show the Hall conductance at $\phi=45°$ over the entire energy spectrum. Around the van Hove singular point of $\Omega=2$, both the longitudinal and Hall conductance reach a maximum. The Hall conductance has changed sign near this point and remains positive for the rest of the energy spectrum. For bond bending of $\approx 2°$, the Hall conductance reaches a maximum value of $\sigma_{xy}^{\text{peak}} \approx \sigma_0$. The longitudinal conductance at this same point is almost identical to the unstretched value, which has been reported elsewhere[13] and reaches a maximum of $\sigma_{xx(yy)}^{\text{peak}} \approx 6\sigma_0 - 8\sigma_0$.

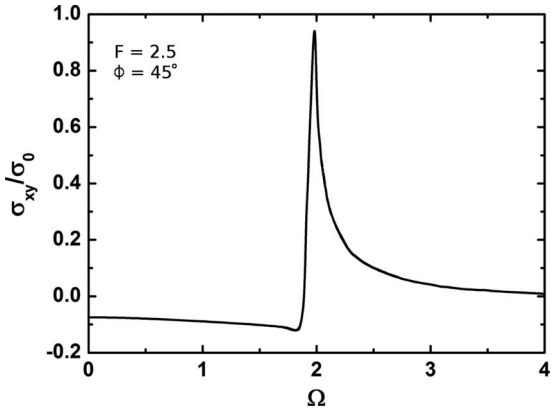

FIG. 4. The transverse (Hall) conductance for $\phi=45°$ and $F=2.5$. The transverse conductance reaches a maximum of $\approx 1\sigma_0$ at the high density of states saddle point $\Omega=2$.

In conclusion, we have calculated the optical conductance of stretched graphene. We have observed a large anisotropy in the universal longitudinal conductance of stretched graphene for small stretching amounts ($\approx$10% anisotropy for bond bending of $\approx 1.16°$). We also have observed that when stretched along chiral directions, the Hall conductance is nonzero, and reaches a maximum value when stretching at an angle of 45° from either the zigzag or armchair direction. Along these two high symmetry directions, however, the Hall conductance was still zero as in intrinsic graphene. The most significant effect of the stretching is that it can induce a Hall conductance of the order of the universal conductance around the van Hove singular point, as well as a sign reversal of the Hall conductance around that same point. Our results provide a method of tuning the optical properties of graphene mechanically.

This work is supported by the Australian Research Council.

[1] K. S. Novoselov, A. K. Geim, S. V. Morozov, D. Jiang, Y. Zhang, S. V. Dubonos, I. V. Grigorieva, and A. A. Firsov, Science **306**, 666 (2004).
[2] A. K. Geim and K. S. Novoselov, Nature Mater. **6**, 183 (2007).
[3] A. H. Castro Neto, F. Guinea, N. M. R. Peres, K. S. Novoselov, and A. K. Geim, Rev. Mod. Phys. **81**, 109 (2009).
[4] K. S. Novoselov, A. K. Geim, S. V. Morozov, D. Jiang, M. I. Katsnelson, I. V. Grigorieva, S. V. Dubonos, and A. A. Firsov, Nature (London) **438**, 197 (2005).
[5] Y. Zhang, Y. W. Tan, H. L. Störmer, and P. Kim, Nature (London) **438**, 201 (2005).
[6] C. Berger, Z. Song, X. Li, X. Wu, N. Brown, C. Naud, D. Mayou, T. Li, J. Hass, A. N. Marchenkov, E. H. Konrad, P. N. First, and W. A. de Heer, Science **312**, 1191 (2006).
[7] H. Suzuura and T. Ando, Phys. Rev. Lett. **89**, 266603 (2002).
[8] S. V. Morozov, K. S. Novoselov, M. I. Katsnelson, F. Schedin, L. A. Ponomarenko, D. Jiang, and A. K. Geim, Phys. Rev. Lett. **97**, 016801 (2006).
[9] D. V. Khveshchenko, Phys. Rev. Lett. **97**, 036802 (2006).
[10] V. P. Gusynin, S. G. Sharapov, and J. P. Carbotte, Phys. Rev. Lett. **96**, 256802 (2006).
[11] A. B. Kuzmenko, E. van Heumen, F. Carbone, and D. van der Marel, Phys. Rev. Lett. **100**, 117401 (2008).
[12] R. R. Nair, P. Blake, A. N. Grigorenko, K. S. Novoselov, T. J. Booth, T. Stauber, N. M. R. Peres, and A. K. Geim, Science **320**, 1308 (2008).
[13] C. Zhang, L. Chen, and Z. Ma, Phys. Rev. B **77**, 241402 (2008).
[14] Z. Q. Li, E. A. Henriksen, Z. Jiang, Z. Hao, M. C. Martin, P. Kim, H. L. Stormer, and D. N. Basov, Phys. Rev. Lett. **102**, 037403 (2009).
[15] T. Stauber, N. M. R. Peres, and A. H. Castro Neto, Phys. Rev. B **78**, 085418 (2008).
[16] K. F. Mak, C. H. Lui, J. Shan, and T. F. Heinz, arXiv:0905.0923v2.
[17] D. S. L. Abergel and V. I. Fal'ko, Phys. Rev. B **75**, 155430 (2007).
[18] A.R. Wright, F. Liu, and C. Zhang, Nanotechnology **20**, 405203 (2009).
[19] A. R. Wright, J. C. Cao, and C. Zhang, arXiv:0905.4304v1.
[20] J. Liu, A. R. Wright, C. Zhang, and Z. Ma, Appl. Phys. Lett. **93**, 041106 (2008).
[21] G. D. Mahan, *Many-Particle Physics* (Kluwer Academic, New York, 2000).